Self-organized gradient hole injection to improve the performance of organic light-emitting diodes

Tae-Woo Lee,* Youngsu Chung, Ohyun Kwon, Jong-Jin Park
**Samsung Advanced Institute of Technology, Mt. 14-1, Nongseo-dong, Giheung-gu,
Yongin-si, Kyeonggi-do, Korea 449-712**
Phone: +82-31-280-6765, Fax : +82-31-280-9349, E-mail: taew.lee@samsung.com

Seoung Wook Chang, Mu-Hyun Kim
**CTO Display R&D Center, Samsung SDI Co., Ltd., 428-5 Gongse-dong, Giheung-gu,
Yongin-si, Kyeonggi-do, Korea 446-577**

Abstract

We demonstrate a new approach to form gradient hole injection layer (HIL) in organic light-emitting diodes (OLEDs). Single spincoating of hole-injecting conducting polymer compositions with a perfluorinated ionomer results in gradient workfunction through the layer by self-organization, which lead to remarkably efficient single layer polymer light-emitting diodes (PLEDs) (~21 cd/A). The device lifetime was significantly improved (~50 times) compared with the conventional hole injection layer, poly(3,4-ethylenedioxy-thiophene)/polystyrene sulfonate. This solution processed HIL also produced dramatically enhanced luminous efficiency (~34 cd/A) in vacuum- deposited green fluorescent OLEDs while the vacuum deposited HIL gave the luminous efficiency of ~23 cd/A in the same device structure.

1. Introduction

Interface engineering between the anode and the emitting layer is important for the improvement of the device lifetime as well as luminous efficiency in PLEDs. Previous literatures reports several approaches to perform interface engineering which results in improvement the device performances of organic light-emitting diodes: (i) anode modification by plasma treatment,[1,2] (ii) chemical modification of the anode,[3-5] (iii) introducing a hole-injection layer (HIL),[6-14] and (iv) a hole transporting interlayer between HIL and emitting layer.[15-17] Hole-injecting conducting polymer films such as polyaniline, polypyrrole, poly(3,4-ethylenedioxythiophene) (PEDOT)[8-11] on indium tin oxide (ITO) layer play important roles to improve the device efficiency and the stability, because they can improve the hole injection from the ITO (workfunction: ~4.7-5.0 eV) and planarize the ITO surface. PEDOT/polystyrene sulfonate (PSS) compositions in aqueous solution are the commercially available well-known Baytron P series HIL materials from H. C. Starck, GmbH.[18] However, PEDOT/PSS has a relatively low workfunction of ~ 5.0 – 5.2 eV[18] so that the hole injection could be a limiting factor in device performance in the case the overlying layer has much lower highest occupied molecular orbital (HOMO) level with respect to the vacuum level. For example, since the HOMO level of poly(9,9-dioctylfluorene) has been estimated to be -5.9 eV[19], the hole injecting energy barrier between PEDOT/PSS and poly(9,9-dioctylfluorene) can be as large as 0.7-0.9 eV. To overcome such a large hole injection barrier between ITO and the HOMO of the emitting layer, a hole injection layer with gradually increasing workfunction from the ITO side toward the emitting layer can be the most appropriate solution. Here, we achieved the fabrication of the HIL with gradient workfunction by self-organization.

Although the device lifetime can be greatly improved by introducing PEDOT/PSS layer, the acidic nature of PEDOT/PSS etches ITO and then indium can migrate into PEDOT/PSS.[20] In addition, recent investigations on failure mode of PLEDs suggested that the polymeric HIL itself can be one of the dominant failure causes.[21] Therefore, at this stage of PLED developments, it is much required to modify HIL to further improve device lifetime as well as device efficiency. In this work, we show that single spin coating of a conducting polymer compositions with a perfluorinated ionomer (PFI) forms a hole injection layer with gradient workfunction by self-organization of the PFI which resulted in remarkably improved device lifetime and efficiency. We formulated a hole injecting conducting polymer compositions composed the commercially available

PEDOT/PSS for OLED application and a PFI. Since the fluorocarbon chains in PFI are more hydrophobic than polystyrene sulfonate, the PFI tends to be preferentially located at the surface of the film by self-organization. Our investigations by AC2 photoelectron spectrometer in air (Riken Keiki Co., Japan) and molecular orbital calculations showed that the higher concentration of PFI resulted in the higher workfunction, and the X-ray photoelectron spectroscopy (XPS) measurement showed that the PFI tends to reside mainly at the upper part of the film. Therefore, the HIL film can have gradient workfunction according to the concentration gradient of PFI in the film, which resulted in remarkable improvement in device luminous efficiency. We also found that the newly formulated HIL with PFI significantly blocks the migration of the In and Sn into the emitting layer by time-of-flight secondary ion mass spectroscopy (TOF-SIMS), which can implies that the HIL layer can act as an appropriate buffer layer for improving the device lifetime.
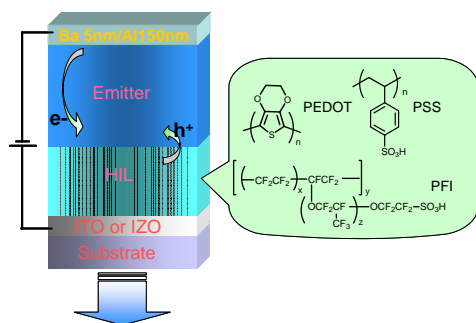
2. Results and Discussion

Figure 1. The PLED device structure and the chemical structures of the components of conducting polymer compositions used for HILs.

Table 1. The workfunction levels of the 5 different conducting polymer compositions.

Sample code	PEDOT/PSS/PFI	Workfunction (eV) (AC2)
AI4083	1 / 6 / 0	5.20
AIPF161	1 / 6 / 1.6	5.55
AIPF81	1 / 6 / 3.2	5.63
AIPF41	1 / 6 / 6.3	5.72
AIPF21	1/ 6 / 12.7	5.79
AIPF11	1 / 6 / 25.4	5.95

Figure 1 shows the chemical structures of the materials we used to formulate our conducting

polymer compositions for the HIL in OLEDs. Commercially available PEDOT/PSS (Baytron P VP AI4083) products in aqueous solution for OLED application were purchased from H. C. Starck. A 5wt% perfluorosulfonate ionomer in mixture of water and alcohol (4.5: 5.5 in volume), was purchased from Aldrich Co. and then it was purified via dialysis using Spectra/Por® CE molecular porous membrane (Cut-off molecular weight: 2000). Baytron P VP AI4083 is composed of PEDOT and PSS at the 1:6 weight ratio which was produced for OLED application due to a low conductivity (6×10^{-4} S/cm). We reformulated the Baytron P VP AI4083 with adding 5 wt% PFI resin. The workfunction levels according to the compositions were measured by ultraviolet photoelectron spectroscopy in air (Surface Analyzer, model AC2, Riken Keiki Co., Ltd). The results are summarized in Table 1. Table 1 shows that the workfunction levels also increase, as the content of PFI increases. Eventually, we obtained a composition with very high workfunction (~5.55-5.95 eV).

Table 2. Calculated dipole moments, ionization potential (IP) and deprotonation energy (DP) of the end groups obtained by density-functional theory calculations.

End Groups	dipole moment[a] (neutral)	dipole moment[a] (deprotonated)	IP (eV)	DP (kcal/mol)
$CH_3CH_2SO_3H$	3.395	4.935	-8.287	336.3
CH_3-O-CH_2SO_3H	4.596	7.159	-7.910	333.7
CH_3-O-$CH_2CH_2SO_3H$	2.681	8.154	-7.424	332.8
$(CH_3)_2CH$-O-CH_2-$(CH_3)CH$-O-$CH_2CH_2SO_3H$	3.807	19.522	-6.943	332.6
$CF_3CF_2SO_3H$	2.800	6.248	-9.316	316.0
CF_3-O-CF_2SO_3H	2.741	7.967	-9.342	315.5
CF_3-O-$CF_2CF_2SO_3H$	2.578	10.107	-9.248	314.4
$(CF_3)_2CF$-O-CF_2-$(CF_3)CF$-O-$CF_2CF_2SO_3H$	2.719	21.940	-9.264	314.3
CH_3CH_2-Ph[b]-SO_3H	2.526	14.596	-7.221	324.9
CH_3CF_2-Ph[b]-SO_3H	3.950	13.310	-8.000	333.3

[a] Debye unit [b] Ph=phenyl

To understand the effect of PFI on the electronic properties of compositions, density functional theory (DFT)[22] calculations were applied to obtain the ionization potential (IP), the deprotonation energy (DP), and the dipole moments of various end groups as shown in Table 2. All calculations were performed at the B3LYP/6-31G(d,p) level by using Gaussian 98 program.[23] We compared the fluorocarbon sulfonic acids with hydrocarbon (alkyl and alkyl substituted benzene (Ph)) sulfonic acids with changing the chain length. The calculated IP level of a fluorocarbon

sulfonic acid is lower than that of corresponding hydrocarbon sulfonic acids (i.e. $CH_3CH_2SO_3H$ vs. $CF_3CF_2SO_3H$). This is because the electron withdrawing ability of fluorine atoms lead to the fact that the fluorocarbon sulfonic acid becomes more difficult to be oxidized than corresponding hydrocarbon one. It is noted that the calculated IP level becomes higher (i.e. closer to the vacuum level) as the alkyl chain length increases but the IP levels are not changed as the fluorinated alkyl chain length becomes longer. This implies that the fluorinated alkyl sulfonic acid in a polymeric form (i.e. PFI) still have lower IP level compared to the corresponding pure alkyl sulfonic acid. When an ether group (-O-) is inserted into the chain, the IP level becomes higher for hydrocarbon sulfonic aicds (i.e. $CH_3CH_2SO_3H$ vs. CH_3-O-CH_2SO_3H) but slightly lower for fluorocarbon sulfonic acids (i.e. $CF_3CF_2SO_3H$ vs. CF_3-O-CF_2SO_3H). When a phenyl group is inserted between alkyl group and SO_3H unit, the IP level becomes higher for both hydrocarbon and fluorocarbon sulfonic acids. These findings suggest that the polymers with the fluorocarbon sulfonic acids such as PFI can also have lower IP levels with respect to the vacuum level than polystyrene sulfonic acids. PFI molecules can be more easily deprotonated than PSS. Calculated dipole moments indicate that the increase of dipole moment ($\Delta\mu$) between neutral form and deprotonated form are larger for fluorocarbon sulfonic acids than corresponding hydrocarbon ones, which leads to the fact that when PFI molecules chemically react with the ITO surface after deprotonation, the holes can be more easily induced by the large dipole moments near the ITO surface. To observe the effect of PFI on the workfunction of ITO surface, we formed a self-assembled monolayer on ITO surface by immersing the UV-ozone-treated ITO into the 0.5wt% PFI solution. Then, it was observed that the water contact angle of the PFI-modified ITO was increased from 55° to 81° which implies the surface became highly hydrophobic and the workfunction was also increased by ~0.5 eV. Judging from all the information above, the high workfunction energy levels in the PEDOT/PSS/PFI compositions can stem from the properties of the PFI itself.

We used XPS to find out surface composition and molecular distribution with depth. Figure 2 shows S 2p spectrum of the film spin cast from Baytron P VP AI4083 aqueous solution. We can deconvolute it with four doublet peaks at 164.5, 166.6, 168.4, and 168.9 eV. We used the energy difference of 1.2 eV between

S $2p_{1/2}$ and $2p_{3/2}$ with a fixed area ratio of 0.5. The doublet peaks at about 169 eV can be assigned to sulfonic acids in the PSS. The components at 168.4 and 168.9 eV correspond to the PSS- salt and PSSH, respectively.[24] The peak at 164.5 eV has been assigned to the sulfur atoms in PEDOT.[24] Besides these, very small peak at about 166.6 eV was added for satisfactory fitting. This peak can be assigned to an intermediate state, sulfone (-SO_2-) between atomic-like sulfur (PEDOT) and SO_3^-.
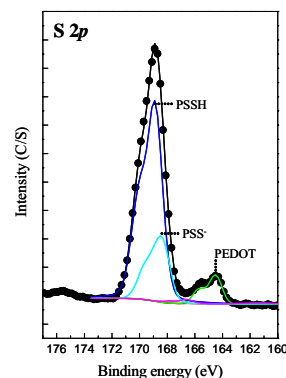

Figure 2. S *2p* core level spectrum a of the conventional PEDOT/PSS (Baytron P VP AI4083).

Figure 3 shows the molecular depth profiles using deconvoluted S 2p peaks with PEDOT, sulfonic acid, sulfone and sulfide. We used the sum of the peak areas of PSSH and PSS- salt to calculate the concentration of sulfonic acid. The sulfide component about at 162 eV increased near the interface with ITO. This may result from the reaction between sulfur and ITO by Ar^+ sputtering during depth profiling. For mixtures of PEDOT/PSS with PFI, we used the C 1s peak at 292 eV to calculate the PFI concentration. This peak can be assigned to CF_2, evidently resulting from PFI.

As shown in the Fig. 3, PSS is a main surface component for conventional PEDOT/PSS and its concentration drops abruptly and shows even bulk distributions until sputter time of 22 min. Due to the increase of sulfide component, the PSS concentration decreases slightly from 22 min, whereas PFI is rich at the surface for the mixtures with PFI and its concentration gradually decreases with depth. We also confirmed that the surfaces of mixtures with PFI were covered with fluorinated carbon using time-of-flight secondary ion mass spectroscopy (TOF-SIMS) as shown in Figure 4.
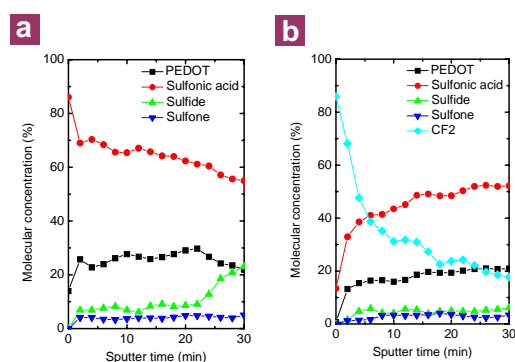
Figure 3. Molecular depth profiles for the HILs of the conventional PEDOT/PSS (a) and the newly formulated PEDOT/PSS/PFI (AIPF41) (b). Deconvoluted S 2p peaks for PEDOT, Sulfonic acid, sulfide, and sulfone concentrations and C 1s peak at 292 eV for PFI concentration were used.

The gradual increase of PFI toward the top surface could make the workfunction increase from the bottom to the top surface. Figure 4 illustrates the schematic energy diagram of the PLED devices to compare the self-organized gradient HIL (Fig. 4b) with the conventional PEDOT/PSS (Fig. 4a). As shown in the Fig. 4b, the HIL has the gradual increase of the workfunction and thus the hole can be efficiently injected into the emitting layer despite of the large energy barrier between ITO and the HOMO level of the emitting layer. We observed that when we fabricated hole-only device with Au cathode, the hole current was much enhanced in the device with PEDOT/PSS/PFI HIL.
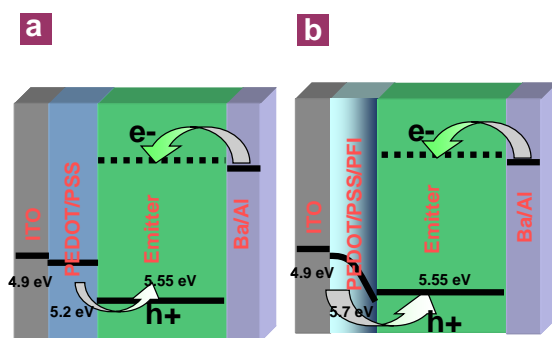

Figure 4. The schematic energy diagram of the devices using the conventional PEDOT/PSS (a) and the PEDOT/PSS/PFI (b) compositions as the HIL.

Figure 5 shows the plots of ^{115}In and ^{120}Sn peaks for the HIL surfaces on ITO measured by TOF-SIMS. The intensities of In (Fig. 5a) and Sn (Fig. 5b) peaks

were greatly decreased when we added the PFI. This indicates the fluorinated surface of new HIL can greatly reduce the diffusion of In and Sn from ITO anode into the emitting layer and therefore act as a diffusion buffer against ITO, which is possibly an important role to improve the device lifetime.
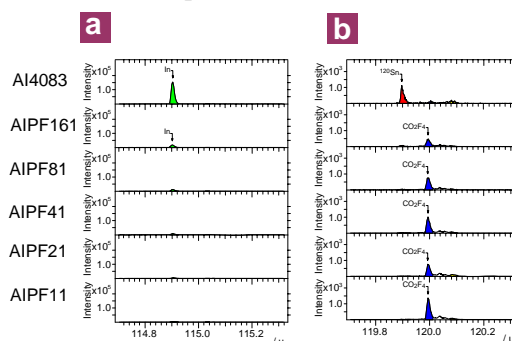

Figure 5. High mass resolution spectra at m/z = 115 and m/z = 200 for 6 conducting polymers with different composition.

We fabricated green-emitting polyfluorene PLEDs by using our conducting polymer compositions (PEDOT/PSS/PFI) as a HIL and compared with the devices by using the conventional PEDOT/PSS (Baytron P VP AI4083). When we fabricated the device using PEDOT/PSS/PFI compositions on ITO (4.9 eV), the maximum luminous efficiency we obtained was 15.1 cd/A which is much higher than that (10.0 cd/A) of the device with PEDOT/PSS (Baytron P VP AI4083). The more improved device efficiency (~21 cd/A) was found in the devices using indium zinc oxide (IZO) anode (5.1 eV) instead of ITO due to the more favorable hole injection from the IZO to the bottom side (>5.1 eV) of the PEDOT/PSS/PFI layer, while the maximum efficiency (9.8 cd/A) of the device with PEDOT/PSS (Baytron P VP AI4083) on IZO was similar to that (10.0 cd/A) of the device with PEDOT/PSS on ITO because the hole injection barrier from PEDOT/PSS into the emitting layer is still high (~0.35 eV). Therefore, as Fig. 6a shows, we compared the device luminous efficiency for the devices using the PEDOT/PSS/PFI composition on IZO with the device using conventional PEDOT/PSS on IZO. The device with PEDOT/PSS/PFI on IZO showed much higher efficiency values (15.2 times @ 100 cd/m^2, 6.3 times @1000 cd/m^2) with function of the luminance than those of the device with PEDOT/PSS on IZO, which resulted from the efficient hole injection from the IZO to the emitter via the PEDOT/PSS/PFI layer and more balanced electron-hole recombination. We tested the

current density of two different hole-only devices (Anode: IZO, cathode: Au) using a PEDOT/PSS/PFI layer or a PEDOT/PSS layer. The device using the PEDOT/PSS/PFI layer showed much higher hole current density than the device using the PEDOT/PSS layer which proves the PEDOT/PSS/PFI layer improves hole injection in PLED devices.
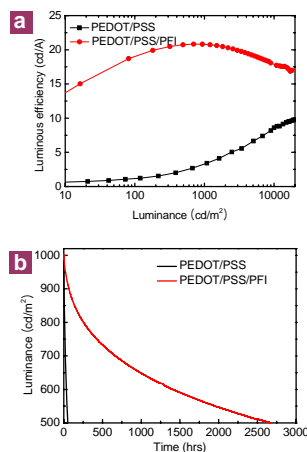
Figure 6. The device luminous efficiency and the device lifetime. (a) The luminous efficiency vs. luminance for the devices using PEDOT/PSS (■) and PEDOT/PSS/PFI (●) as the HIL in the structure of IZO/HIL/green emitter/Ba/Al. (b) The device lifetime with initial luminance 1000 cd/m^2 for the devices using PEDOT/PSS.

We also tested the device lifetime of the device using PEDOT/PSS/PFI at initial luminance 1000 cd/m^2 after 5 min aging at 1000 cd/m^2 as shown in Fig. 6b. The half-lifetime (2680 hrs @ 1000 cd/m^2) of the device using PEDOT/PSS/PFI was dramatically improved compared with the half-lifetime (52 hrs @ 1000 cd/m^2) of the device using PEDOT/PSS. The device efficiency and the accelerated lifetime at 1000 cd/m^2 we obtained when the emitting polymer film was baked at 100°C are reasonable values according to the previous literature for the devices of a green-emitting polyfluorene derivative.[25,26] Therefore, the remarkable improvement indicates that the compositions including perfluorinated ionomers can be one of the promising hole-injection buffer materials for enhancing the device lifetime. Since the fluorocarbon sulfonic acids in the HIL are preferentially reside on the film surface, it can effectively block the impurities stemming from the PEDOT/PSS and ITO (alkali metal, sulfate, In, Sn and etc). The fluorocarbon has intrinsically a good chemical stability and hydrophobicity. In fact, our HIL materials are less sensitive to the moisture

relative to the conventional PEDOT/PSS. In this respect, the greatly improved lifetime can be ascribed to the effective diffusion barrier characteristics of the PFI as well as the improved balanced electron-hole recombination by gradient hole injection resulting in a lower driving current density at the same luminance. We are still trying to further improve the lifetime by optimizing the film annealing temperature and the device structures such as electrode structure and thickness, and by using purified PEDOT/PSS and PEDOT/PSS/PFI.
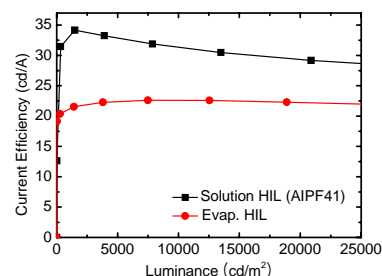
Figure 7. The device luminous efficiency of vacuum deposited green fluorescent OLED device using solution processed and vacuum deposited HILs. Except for the HILs, layer structures in the devices are same.

We also employed the HIL (AIPF41) in vacuum-deposited green fluorescent OLEDs. Although commercially available vacuum-deposited HIL showed the luminous efficiency of ~23 cd/A, the solution processed HIL produced a dramatically enhanced luminous efficiency of ~34 cd/A in the same device structure (Fig. 7), which is the highest value in fluorescent OLEDs to the best of our knowledge.

3. Conclusion

We found that the single layer of the conducting polymer compositions including perfluorinated ionomers produces gradient workfunction by self-organization, which can be the most appropriate solution to overcome the large energy barrier for hole injection between the indium-tin-oxide and the HOMO of the emitter in PLEDs. We achieved remarkably enhanced luminous efficiency (~21 cd/A) even in singly layer PLEDs and dramatically improved device lifetime (~50 times) using the conducting polymer compositions containing a perfluorinated ionomer compared with the conventional poly(3,4-ethylenedioxythiophene) /polystyrene sulfonate. Even compared with recent data of maximum luminous efficiency (12.3 cd/A) for

green PLEDs by Sumitomo Chemical Co., the luminous efficiency we achieved is the remarkably high value in fluorescent green PLEDs. The achieved lifetime was 2680 hours at the initial luminance 1000 cd/m^2 which corresponds to the 169000 hours at the initial luminance of 100 cd/m^2 when we estimated by using the 1.8 power number for acceleration test, which is one of the state-of-art results. These results can be a good example demonstrating that the shorter lifetime of PLEDs compared with the SM-OLED is not mainly due to the inherent degradation of polymeric emitter itself. Hence, our results will light up the possibility of further great improvement of PLEDs for the real applications to large area and full-color flexible displays with long lifetime.

In addition to the great improvement in luminous efficiency and device lifetime in PLEDs, the employment of our HILs in vacuumed deposited small molecule OLEDs leads to greatly enhanced performance. This solution processed HIL also produced remarkably enhanced luminous efficiency (~34 cd/A) in vacuum-deposited green fluorescent OLEDs, while the vacuum deposited HIL gave the luminous efficiency of ~23 cd/A in the same device structure. The highly enhanced luminous efficiency in OLEDs will greatly reduce the power consumption in consumer electronic displays.

Furthermore, the controllability of the workfunction of these compositions can be widely used for charge-injecting contact to improve the device performance in other various organic electronic and optoelectronic devices.

4. References

[1] J. S. Kim, R. H. Friend, and F. Cacialli, Appl. Phys. Lett. **74**, 3084 (1999).

[2] J. X. Tang, Y. Q. Li, L. R. Zheng, and L. S. Hung, J. Appl. Phys. **95**, 4397 (2004).

[3] B. Choi, J. Rhee, and H. H. Lee, Appl. Phys. Lett. **79**, 2109 (2001).

[4] S. Kato, J. Am. Chem. Soc. **127**, 11538 (2005).

[5] Q. Huang, G. Evmenenko, P. Dutta, P. Lee, N. R. Armstrong, and T. J. Marks, J. Am. Chem. Soc. **127**, 10227 (2005).

[6] S. Kim, C. Hsu, C. Zhang, H. Skulason, F. Uckert, D. LeCoulux, Y. Cao, and I. Parker, J. Inf. Disp. **5**, 14 (2004).

[7] T.-W. Lee, O. Kwon, M.-G. Kim, S. H. Park, J. Chung, S. Y. Kim, Y. Chung, J.-Y. Park, E. Han, D. H. Huh, J.-J. Park, and L. Pu, Appl. Phys. Lett. **87**, 231106 (2005).

[8] Y. Yang, E. Westerweele, C. Zhang, P. Smith, and A. J. Heeger, J. Appl. Phys. **77**, 694 (1995).

[9] R. W. T. Higgins, N. A. Zaidi, and A. P. Monkman, Adv. Func. Mater. **11**, 407 (2001).

[10] S. A. Carter, M. Angelopoulos, S. Karg, P. J. Brock, and J. C. Scott, Appl. Phys. Lett. **70**, 2067 (1997).

[11] J. Gao, A. J. Heeger, J. Y. Lee, and C. Y. Kim, Synth. Met. **82**, 221(1996).

[12] M. Gross, D. C. Müller, H.-G. Nothofer, U. Scherf, D. Neher, C. Bräuchle, and K. Meerholtz, Nature **405**, 661 (2000).

[13] P. K. H. Ho, J.-S. Kim, J. H. Burroughes, H. Becker, S. F. Y. Li, T. M. Brown, F. Cacialli, and R. H. Friend, Nature **404**, 481 (2000).

[14] A. Elschner, F. Bruder, H.-W. Heuer, F. Jonas, A. Karbach, S. Kirchmeyer, S. Thurm, and R. Wehrmann, Syn. Met. **111-112**, 139 (2000).

[15] J. H. Burroughes, Asia Display/IMID'2004, 23-27 August, Daegu, Korea, session 11.4 (2004).

[16] J.-S. Kim, R. H. Friend, I. Grizzi, and J. H. Burroughes, Appl. Phys. Lett. **87**, 023506 (2005).

[17] H. Yan, P. Lee, N. R. Armstrong, A. Graham, G. A. Evmenenko, P. Dutta, and T. J. Marks, J. Am. Chem. Soc. **127**, 3172 (2005).

[18] The material information is available in the H.C. Starck website, http://www.hcstarck.com/.

[19] S. Janietz, D. D. C. Bradley, M. Grell, C. Giebeler, M. Inbasekaran, and E. P. Woo, Appl. Phys. Lett. **73**, 2453 (1998).

[20] M. P. de Jong, L. J. van IJzendoorn, and M. J. A. de Voigt, Appl. Phys. Lett. **77**, 2255 (2000).

[21] X. Crispin, S. Marciniak, W. Osikowicz, G. Zotti, A. W. denier van der Gon, F. Louwet, M. Fahlman, L. Groenendaal, F. de Schryver, and W. R. Salaneck, J. Polym. Sci. B: Polym. Phys. **41**, 2561 (2003).

[22] W. Koch and M. C. Holthausen, A Chemist's Guide to Density Functional Theory; Wiley & Sons, New York (2000).

[23] M. J. Frisch et al., Gaussian 98 Rev. A.9; Gaussian, Inc., Pittsburgh, PA (1998).

[24] G. Greczynski, Th. Kugler, and W. R. Salaneck, Thin Solid Films **354**, 129 (1999).

[25] J. Kim, J. Lee, C. W. Han, N. Y. Lee, and I.-J. Chung, Appl. Phys. Lett. **82**, 4238 (2003).

[26] M. C. Suh, H. K. Chung, S.-Y. Kim, J. H. Kwon, and B. D. Chin, Chem. Phys. Lett. **413**, 205 (2005).